75th International Astronautical Congress (IAC), Milan, Italy, 14-18 October 2024.

IAC-24-C2.8.3,x88135

Additive Manufacturing of Space Propulsive Components: Characterization of IN718 Powder Recycling on Final Samples Properties

Davide Zuin[a*], Simone La Luna[a], Ludovica Cavallucci[a], Filippo Maggi[a]

[a] *Department of Aerospace Science and Technology (DAER), Politecnico di Milano, Via La Masa 34, Milan, Italy*
* Corresponding Author, davide.zuin@polimi.it

Abstract

The recent proliferation of Additive Manufacturing (AM) technologies is primarily led by their possibility of printing complex shapes that would not be feasible with conventional subtractive methods. Although their widespread diffusion in the aerospace market, standardization challenges associated to these productions are still lacking. These activities are necessary, in particular when dealing with critical parts such as space propulsion components associated to strict quality assurance requests. This necessity becomes even more pronounced when considering recycled metal powder for AM applications in critical space components.

The present work focuses on the characterization of recycled powders and samples printed through AM Selective Laser Melting (SLM). The work is based on the evaluation of a design of experiment (DoE) exploring the manufacturing cycle of space propulsive components. Starting from the characteristics of the machines and facilities involved in the experimental setup, the focus is shifted towards a state-of-the-art analysis of AM characterization methodologies for space applications parts. The definition of the experiment is proposed: the aim of the DoE is the evaluation of modifications to as printed components properties when manufactured with recycled powders up to 11 recycles. Both mechanical properties and dimensional characteristics are evaluated: the first through dedicated samples, while the latter through the definition of a specific test artefact. Results from the DoE confirm previous literature data and show the consistency of the applied recycling method for the manufacturing of space critical components.

Keywords: Additive Manufacturing, Selective Laser Melting, powder recycling, Inconel 718, surface properties, mechanical performances.

Nomenclature

L_c	Cut-off length
L_t	Total length
n	Number of measurements
Ra	Average surface roughness
SD	Standard deviation
X	Individual measurement
$\bar{x}$	Average measurement
δ	Layer thickness
θ	Inclination angle

Acronyms/Abbreviations

AM	Additive Manufacturing
AMP	Additive Manufacturing Procedure
AMVP	Additive Manufacturing Verification Phase
ASTM	American Society for Testing and Materials
CMM	Coordinate Measurement Machine
DAER	Department of Aerospace Science and Technology at Politecnico di Milano
DED	Direct Energy Deposition
DoE	Design of Experiment
ECSS	European Cooperation for Space Standardization
HFP	Hardware Fabrication Procedure
HP	Hardware Production
IN718	Inconel 718
ISO	International Organization for Standardization
L-PBF	Laser Powder-Bed Fusion
OOS	Out of Specification
PVP	Prototype Verification Phase
SLM	Selective Laser Melting
SPLab	Space Propulsion Laboratory

1. Introduction

Additive Manufacturing (AM) is a key enabling technology that allows to print components layer-by-layer typically using powder or filament as feedstock, which is melted by a focused heat source and then cooled to form the final part. AM has facilitated rapid prototyping and production of consistent long-term components, making it applicable across various sectors, including aerospace. In fact, elements built through AM not only exhibit complex geometries but are also lighter and stronger than those produced by conventional manufacturing methods [1].

Common materials in AM are metals in pulverized form, such as nickel-based superalloys, valued for their strength, corrosion resistance, and ability to withstand high stress and temperature conditions. When dealing with metals in powder conditions, the unused material from a printing cycle can be employed in subsequent cycles after the implementation of specific

postprocessing. Powder recycling refers to the process of refurbishment of the powder after a printing step to create the feedstock for new jobs. The process leverages on different strategies, as defined by literature [2]. The main ones are called continuous powder refreshing from the original powder lot, or collective ageing of the entire powder sample. Powder reusing is performed until some of the powder properties reach Out of Specification (OOS) limits, indicating powder degradation, or until there is insufficient material to complete the next build cycle [3]. During reuse post-processing, powder properties shall be restored to the original ones from the virgin lot. This can be achieved by sieving and gradually removing deformed particles and sintered agglomerates, or by mixing old and virgin powder, thus extending the material lifespan but at the cost of losing traceability. These approaches can offer potential savings from both environmental and economic perspectives.

AM applications are still not widespread in the industrial landscape due to significant challenges. Among these challenges, definition of qualification criteria for AM processes based on the produced objects quality is a key factor [4]. Issues such voids or anisotropy may occur and negatively impact the mechanical properties. Poor results in terms of accuracy and final part quality may force the addition of expansive and time-consuming post-processing activities, thereby losing the benefits of AM compared to conventional manufacturing techniques [5, 6]. This issue is mainly present when few post-processing activities are expected by design: the work from Gradl et al. shows that there may be a significant issue when dealing with L-PBF techniques, which could involve in some cases multiple post-processing steps compared to other AM technologies [7]. To reduce the impact of the post-processing activities within the product manufacturing lifecycle, careful selection of process parameters and part orientation is needed.

In these terms, norms and standards still lack a full comprehensive set of guidelines and strategies to achieve a proper comprehensive set of machine parameters able to deliver high-quality space parts. Tailored standards are needed to ensure that production and operational outcomes consistently fall within acceptable limits, especially for critical components in space applications. In order to properly characterize final built parts, testing activities on final samples printed together with the requested parts must be conducted to verify that specific criteria are met and to ensure the acceptability of both the process and the product. Furthermore, the introduction of specific geometric samples within dedicated artefacts has been considered within previous literature studies [8].

Within the framework of the SPLab, a series of activities involving AM SLM of space propulsive components for high-temperature/high-oxidation resistance has been developed. For this purpose, a Concept Laser M2 machine with a single laser operating in continuous mode has been used. The involved high-strength/high-resistance powder selected has been Inconel 718 (IN718). The aim of this work is the definition of a qualification campaign aimed at the evaluation of IN718 samples and their properties.

The samples have been printed with increasingly recycled powders, from virgin lot up to 11 times. Powder recycling is achieved through a sieving process with a particle size threshold of 63 µm. To ensure reusability up to the 11th reuse, a proportional blend with virgin particles is added at each stage of the process. The applied standard for the overall DoE is based on a specific tailoring of the ECSS-Q-ST-70-80C [9]. From the standard, a qualification test plan has been established to validate the SLM technology, the machine and the IN718 powder recycling method adopted to produce the components.

2. Test Plan Description

The qualification test plan is based on a sequence of JOBs, defined as a group of samples with specific geometries and powder conditions. Samples are printed according to a series of steps defined in an Additive Manufacturing Procedure (*AMP*). Each JOB refers to a dedicated verification phase as expressed in the ECSS standard, namely Additive Manufacturing Verification (*AMVP*) plan and Prototype Verification (*PVP*) plan.

The complete organization of the JOBs and their characteristics is reported in Table 5 in Appendix A. Within the phases, quantitative analyses were performed on artefacts and samples from each JOB. Metallographic and densification observations were made on cubic specimens to study the evolution of pores distribution after the printing cycles; tensile testing was carried out on cylindrical heat-treated samples to examine the effects of recycling on mechanical behaviour; dimensional errors and roughness values were collected on samples of various geometries, retrieved from the test artefact, to check the status of external as-printed surfaces.

2.1 Printed Samples Organization

An example of printing job configuration is depicted in Figure 18 in Appendix A. Each layout featured several identical specimens placed at different positions on the building job to evaluate the effects of orientation and location on the final sample property under analysis. In certain JOBs, a powder capture sample, shaped as a cone, was included to contain enough material for tests to assess powder properties, as outlined in the standard [9].

The first step of the qualification test plan involved a pre-verification phase with the aim to identify the proper machine parameters and printing strategy for the DoE. This phase included JOB0, JOB0.1, JOB 0.2, JOB1 and JOB1.1: within these prints, rectangular specimens (or process benchmarks) made of virgin powder were considered. This phase was used to select the most

optimal process parameters for the adopted skin-core scanning strategy through measurements of the average surface roughness, material densification values, porosity and defects on micrographic section and other tests. The selected parameter results from these previous analyses are reported in Table 1.

The *AMVP* phase started with JOB2 and JOB3, still made from virgin powder, but including geometric and mechanical benchmarks, such as cylindrical specimens also destined to mechanical testing.

2.2 Test Artefact

Starting from JOB4, the layout started including a test artefact for the evaluation of recycling steps effects on different geometrical features. The test artefact, called "Test Cube", is briefly reported in Figure 1.

The design of the test cube takes its steps from the evaluation of standard ISO/ASTM 52902:2019(E) [10] and the identification of common features for SLM machine benchmarking. The selected shapes and dimensions are made to evaluate the AM machine and the production in terms of accuracy, resolution and surface texture across multiple recycling steps. This process is defined to find printing limitations reached when operating at specific process parameters. The assumed configuration of the artefact has been selected for spatial optimization and to facilitate dimensional measurements before disassembling the Test Cube for other studies.

The *PVP* includes the specimens from JOB4 to JOB14, which recall the same organization of JOB3 (except for JOB5, which does not contain the Test Cube) and powder reused at each new printing cycle. The last group, JOB15 with 11x recycles, is designated as fully representative of the sequent Hardware Production (HP) phase; this print shall be correlated to a dedicated Hardware Fabrication Procedure (HFP) covering both this and the previous JOBs. The final job includes full representative components to be printed after acceptance of the recycling results coming from the previous phase testing activities.

3. Process and Analyses

A common additive manufacturing procedure was settled for the JOBs, covering all the aspects associated to the SLM process. The procedure, resumed in the Additive Manufacturing Procedure (AMP) document, includes some specific postprocessing operations, which all the samples designated for mechanical analyses underwent.

After sample platform cutting, stress relief was performed to eliminate distortion and reduce internal stresses; then, solubilization followed by air cooling, to minimize the eventual defects caused by the manufacturing process (e.g. melt pool boundaries) and to dissolve Laves-phases, which are generally associated with reduced mechanical properties; afterwards, aging to promote the formation of stable γ and γ′′ phases, enhancing strength in the material; finally, air cooling of all samples.

Table 1: Body and contour process parameters selected for the printing.

Parameter	*Body*	*Contour*
Spotsize, [μm]	130	50
Power, [W]	250	120
Scan Speed, [mm/s]	800	1200
Hatch Spacing, [mm]	0.10	-
HZB, [mm]	-	0.080
Layer Thickness [μm]	25	
VED [J/mm^3]	125	-

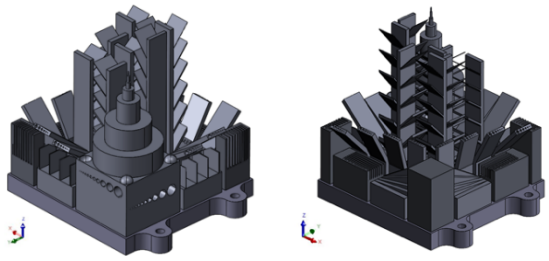

Figure 1: Test artefact, or "Test Cube", CAD model.

These postprocesses were accompanied by other passages, such as ultrasonic cleaning and Computer Numerical Control machining, where needed. The heat treatment steps are crucial not only to confirm the high strength reported by samples produced by a SLM machine but also to determine whether factors impact the material's properties, such as powder recycling, temperature, printing orientation, and post-processing. It is worth noticing that the test artefact was not subjected to these properties, not to alter the characteristics of the sample itself.

Mechanical tests were included on heat-treated samples. Cylinders were printed and reworked for mechanical tests: the organization of the cylindrical specimens used for testing is presented in
Table 2.

Metallographic and micrographic observations were executed to examine the distribution of porosity resulting from the adopted process approach and parameters, as well as the changes in the Inconel 718 particles over 11 reuses. The aim was to understand how defects manifest over time, particularly with repeated powder recycling, and how the outputs of the analyses are affected.

Table 2: Tensile tests samples organization.

Parameter	Body	Contour
9 (x-direction) 9 (y-direction) 9 (z-direction)	12x90 mm^2	JOB1
20 (z-direction)	12x140 mm^2	JOB2
20 (z-direction)	12x140 mm^2	JOB3
10 (z-direction)	12x140 mm^2	JOB4
10 (z-direction)	12x140 mm^2	JOB5
10 (z-direction)	14x140 mm^2	JOB6-JOB15

Table 3: Artefacts classification and evaluation index according to standard [10].

Evaluation Index	*Artefact*	*Characteristics*
Accuracy	Linear	Position, straightness
Resolution	Holes	Diameter, depth, cylindricity
	Ribs	Thickness, straightness
	Slots	Width, flatness, parallelism
Surface Texture	Surface roughness	Average roughness

Analyses at test artefact level were considered as well. The standard [10] introduces several indices that shall be analysed on the secondary artefacts of the test cube: linear and circular accuracy, resolution of holes, slots and ribs, and surface texture. Table 3 lists the characteristics to be measured, for each secondary artefact. Linear artefacts are useful to evaluate linear positioning precision in a specified direction, while circular artefacts highlight potential defects caused by the material. Resolution holes aid in determining the smallest achievable hole size; resolution ribs define the minimum achievable wall thickness, either straight or inclined; resolution slots identify the minimum feature spacing. Finally, assessment of surface texture is necessary to understand the final superficial quality obtained directly from the production process.

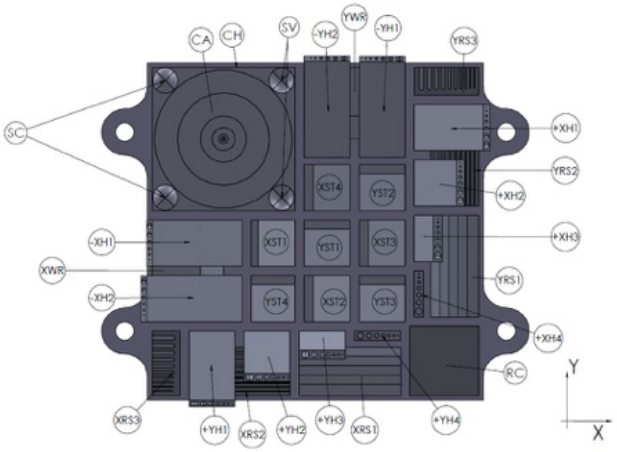

Figure 2: Test artefact features with corresponding labels, as seen from the XY plane.

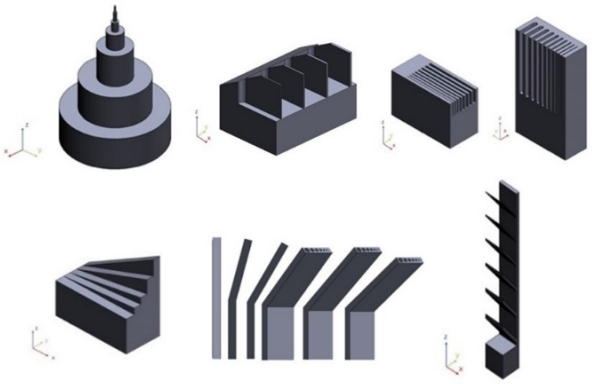

Figure 3: Some artefacts extracted from the Test Cube. From top left to bottom right: concentric cylinders and resolution pins, resolution walls, resolution slots, resolution slotted angles, resolution holes, samples for surface texture evaluation.

The correspondence between the shapes described by the standard and the Test Cube artefacts (labelled according to a specific convention, visible in Figure 2) is indicated in the following list:

- Linear Artefacts:
  - Reference Cube RC
- Circular Artefacts:
  - Semi-spheres, two concave (SC) and two convex (SV).
  - Concentric cylinders CA with nominal diameters of 30.0, 20.0, 10.0, 5.0, 2.0, 1.0, 0.5 mm.
- Resolution Artefacts:
  - Resolution walls XWR/YWR, considering a thickness which goes from 0.2 to 0.5 mm.
  - Resolution holes ± X/YH, with channels of different diameters printed on walls with

varying inclinations that go from 35° to 90°.
  - Resolution slots X/YRS 2 and 3, with a spacing in the range 0.1-0.8 mm, and 0.1-1.0 mm respectively.
  - Resolution slotted angles X/YRS, with inclined thin surfaces ranging from 0° to 30°.
- Flat surfaces of varying thicknesses and inclinations for surface texture evaluations called X/YST towers.

Some of these artefacts are singularly illustrated in Figure 3.

To verify the overall process, dimensional errors analysis was performed by a Coordinate Measurement Machine (CMM) and by a feeler gauge, in conjunction with surface roughness measurements carried out with a TESA-Rugosurf 20. This electronic instrument is equipped with a diamond-like stylus that moves in contact with the surface texture at a speed of 1 mm/s to capture detailed surface texture data.

4. Procedures

Procedures of tests samples included test procedures derived from standards and available technical notes on testing of samples in AM. These procedures are listed in the following sections.

1.4 Mechanical Tensile Test

The uniaxial tensile test was performed according to standard ASTM E8/E8M [11], at room temperature. Not all samples were tested: a selection of representative specimens was chosen, specifically those printed in key peripheral positions where powder distribution plays a critical role. The test results were compared to reference values from ISO 6892 [12] for heat-treated specimens, which specify a tensile strength of approximately 1250 MPa, a yield strength of 950 MPa, and an elongation of 12%.

1.5 Metallographic and Micrographic Test

For each JOB, four cubic samples (15x15x15 mm³) built along the z-axis were analysed to assess the porosity evolution. The samples, labelled as A1, A5, B1, B5, differed in heights and positions on the building plate, allowing a comparative evaluation.

Two methods were employed for the analysis:

- Density measurement by immersion method, conducted according to ASTM B311 REV.17 [13], to provide an overall density measurement of the samples.
- Porosity estimation via micrographic examination on polished sections parallel to the build direction, following ASTM E3 Rev 11 (2017) [14] and ASTM E407 Rev 2023 [15] standards. Five fields of view, each at 50x magnification, were examined within areas of approximately 1.5x2.0 mm² (Figure 4). An

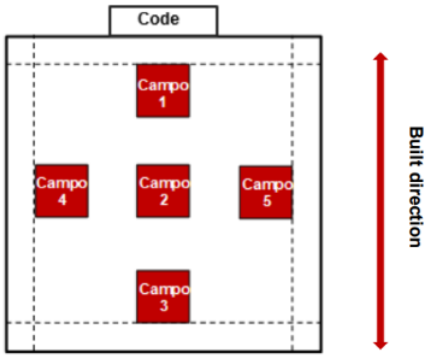

Figure 4: Indication of the five fields on a metallographic sample section.

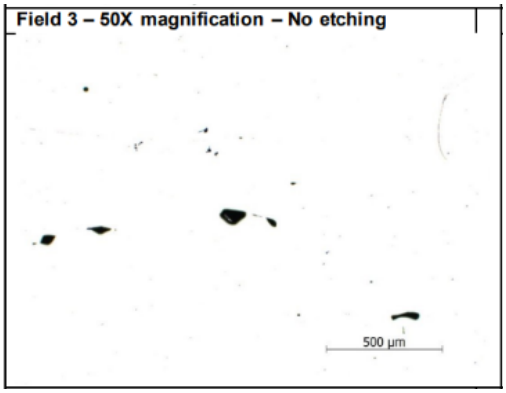

Figure 5: Micrographic field n.3, as recovered from sample A5 on JOB8.

image analysis software was used to quantify the voids content by distinguishing the contrast between metal (light shade) and voids (dark shade), as visible in Figure 5. For each field, the relative density was calculated, and the average of the five fields provided an estimate of the porosity for the entire sample. It was therefore assumed that the voids observed in the surface sections were representative of the porosity distribution throughout the sample.

4.3 Dimensional Error Measurement

To assess the printing performance of the SLM machine, dimensional errors – defined as deviations from the intended geometries – were measured. These measurements served to identify unprintable shapes and dimensions due to factors such as process parameters, powder recycling, artefact orientation, machine capabilities, and their combined effects. The measurements executed on the Test Cube followed the guidelines of the ISO/ASTM standard, which specifies the evaluations applicable for a geometrical piece.

Table 4: Artefacts, measurement types and methods according to ISO/ASTM 52902:2019(E).

Artefact	*Measurement Method*	*Measurement Type*
RC	CMM	Height, flatness, width, parallelism, perpendicularity
CA	CMM	Height, diameter, parallelism, concentricity, cylindricity
SV, SC	CMM	Sphericity, diameter
±XH, ±YH	CMM	Flatness, inclination
XWR, YWR	CMM	Height, flatness, walls width and distance
XRS, YRS	CMM Feeler gauge	Height, inclination, flatness, slot width
XST, YST	CMM	Inclination, wall distance and thickness, width, height

To enable the operation of the CMM, a total of 185 planes were designed and referred to all the exposed faces of the artefacts, including circular surfaces and semi-spheres. Slot thickness measurements were performed using a feeler gauge, a tool consisting of small lengths of steel with thicknesses ranging from a sensitivity of 0.05 mm to 1.0 mm, with an increment of 0.05 mm. If the gauge could fit into the slot, it was recorded as a "Pass", otherwise it was marked as "No-Pass". The corresponding value of steel length indicates the effective achieved thickness, thus the nominal dimension was determined by comparing the measured value with the intended dimension, and calculating the difference.

4.4 Surface Roughness Measurement

The instrument collects values to compute the average surface roughness Ra according to the formula:

$$Ra = \frac{1}{L_t}\int_0^{L_t} z(x)\,dx \quad (1)$$

where L_t reports the length of measurement along z direction.

To set up the surface roughness measurement, two fundamental parameters need to be defined: the cut-off length, which is the sampling length, and the number of cut-offs, referring to how many times that length is consecutively repeated, determining the total run covered by the probe. Parameter settings are typically guided by standard protocols: according to ISO 3274 [16] – the reference standard for the instrument – the cut-off length is selected according to the expected surface roughness. For a L-PBF technology, the average surface roughness is generally within a range of $Ra = 2 - 10$ µm [17], thus the cut-off length has been selected with a value of 2.5 mm. The recommended number of cut-offs from the standard is 5, but if the resulting path is excessive for the piece undergoing measurement, then this value can be reduced in function of what is expressed by equation (2), where L_t reports the total length and L_c the cut-off one:

$$L_t = (number\ of\ cut - offs + 1) \times L_c \quad (2)$$

In this analysis, for many surfaces, the total length exceeded practical limits even after reducing the number of cut-offs. As a result, the number of cut-offs was maintained at 5, but L_c was reduced to 0.8 mm. It is noted that deviating from the standard guideline may lead to less accurate results: for example, a reduction in Ra by 9.86% was observed when comparing values obtained from the same surface (straight back walls of towers X/YST) first with L_c = 2.5 mm, and then with 0.8 mm.

The main objective of this part of the analysis was to observe roughness evolution with powder recycling: when powder is recycled, alterations may occur, due to uncontrolled agglomerations, creating larger-sized particles that are more resilient to melting [18]. To provide a clearer understanding of the results, each average surface roughness for a particular JOB (representing a specific powder reuse cycle) is coupled with a standard deviation (SD) value, calculated using Equation (3), where X represents the individual measurements, $\bar{x}$ their average, and n the number of measurements:

$$SD = \sqrt{\frac{\sum(X-\bar{x})^2}{n-1}} \quad (3)$$

5. Results and Discussion

Samples were tested separately considering the tensile and mechanical specimens first and then dimensional and surface roughness specimens. Therefore, results are reported and commented separately in this section.

5.1 Tensile Test Result

Tensile test results are consistent with literature data on recycled IN718 tensile samples after heat treatment

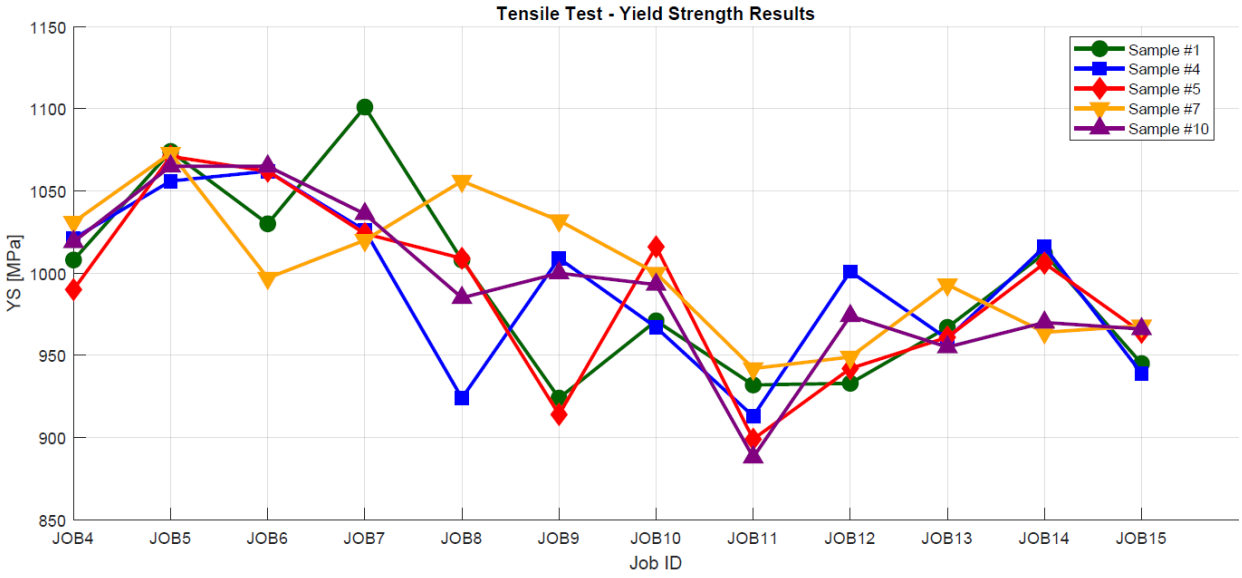

Figure 6: Tensile test results, yield strength.

[19]. Regarding the tensile resistance, no significant difference was observed up to JOB7 (3x recycled powders): the minimum value is reported around 1255 MPa, while the maximum is registered at 1350 MPa. Starting from JOB8, however, there was a slight decline, with values oscillating between 1200 and 1300 MPa. This decrease was not uniform, as JOB14 showed values similar to those of earlier JOBs, before dropping again in the final print.

The same trend is observed for yield strength, which ranges from 900 MPa to 1100 MPa, as reported in Figure 6. In JOB7, a peak value of 1101 MPa was recorded, but there is a noticeable decreasing trend as the feedstock is reused more times. JOB11 results are consistently lower than the others, as all values reported are below 950MPa. The aforementioned results in terms of mechanical behaviour can be justified primarily by the powder recycling phenomenon, which is the only independent variable as the same process, printing orientation, sampling and postprocessing is kept for all specimens. It shall be noted that, although the slight modifications, all values remained above 900MPa and did not show significant differences between JOBs, even though the high number of recycling steps.

5.2 Metallographic and Micrographic Test Results

Metallic matrix metal matrix of austenitic γ phase microstructure and dispersion of precipitates with columnar distribution was observed for all samples. Defects were observed in all micrographic images of the JOB samples, as small pores were usually distributed across all the analysed surfaces. This is a typical result for AM SLM of IN718 materials. The distribution of pores was even across the five fields for all specimens.

An important aspect of the postprocessing of the internal defects is associated to the presence of irregular porosities, which tends to increase with the number of powder reuse.

Densification values, measured through immersion method and through metallographic analysis, gave comparable and consistent results, the trends were largely aligned, indicating similar behaviour for both evaluation types. Nevertheless, this was not always the case; in certain JOBs, the profiles were not consistent across the two measurements. This suggests that the evolution of porosity does not follow a predictable trend, as density values fluctuated step after step, disorderly and probably influenced by flowability and packing capability. Nonetheless, porosities values above 99% for all samples across all recycling steps were retrieved.

5.3 Dimensional Error Results

Measurements conducted using the CMM revealed deviations from nominal values, showing both under-sizing and oversizing in the features. While most of results fell within the tolerance range specified by the ISO/ASTM standard, some dimensions and shapes exhibited errors exceeding the allowable maximum and minimum tolerances. The deviations can be attributed to various factors, including difficulties in measuring small and thin surfaces with the CMM, and printing issues related to the SLM machine.

An example of this case can be reported when considering the result assessment of *resolution pins* (CA samples) across recycling steps, as reported in Figure 7. Pins with a diameter of 0.5 mm were too small to be measured, while 1.0 mm – although measurable – highlighted out-of-bounds results pointing towards an improper data collection. It is important to highlight that

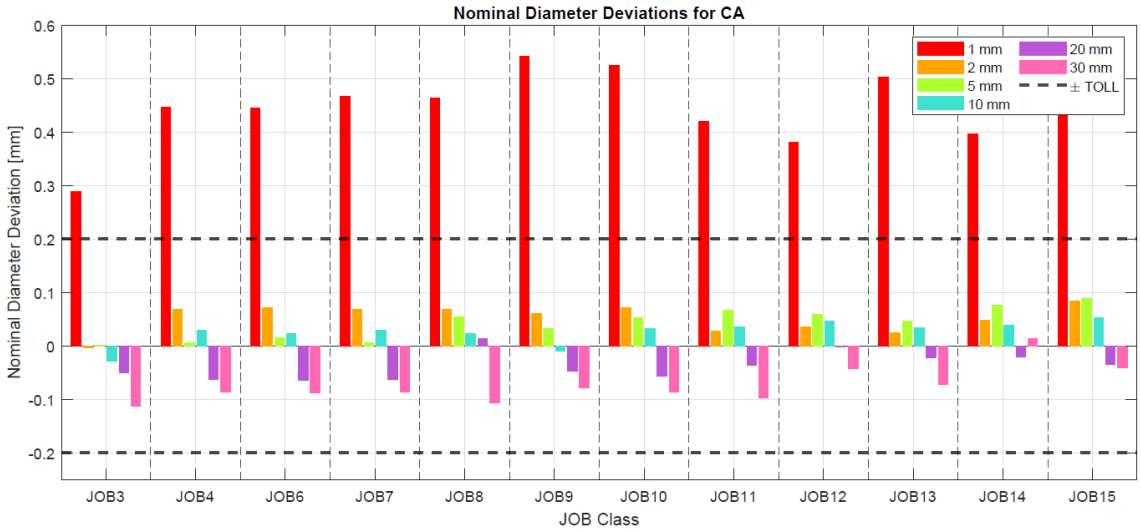

Figure 8: Diameter deviation trends for CA.

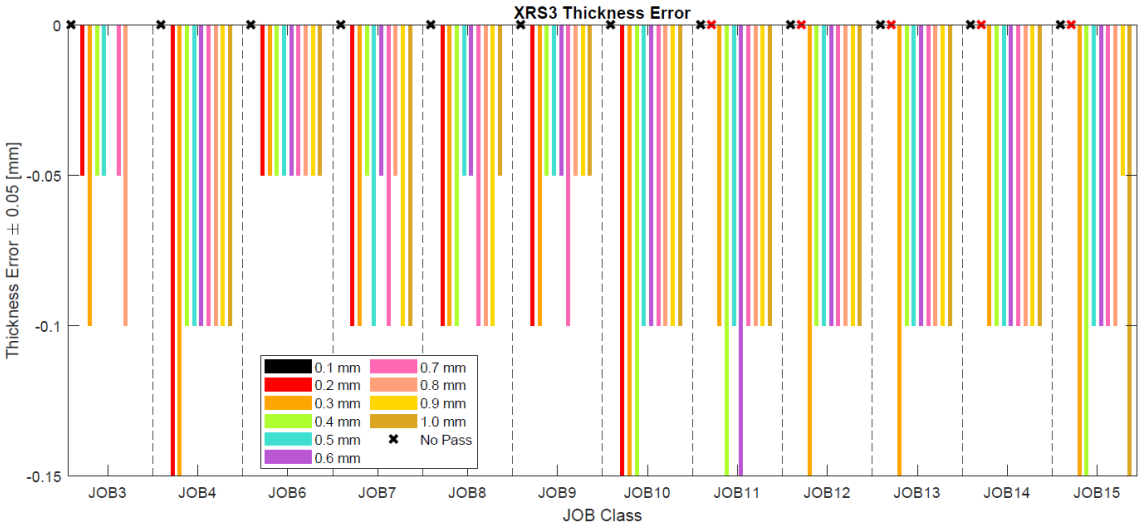

Figure 7: Slot thickness deviations for XRS3.

no significant changes along recycling steps are measured on this feature. Furthermore, dimensions of all pins are well within the standard margins (±0.2 mm).

When considering results from the *resolution slot* (XRS/YRS samples) part, issues in terms of SLM are highlighted. These data, retrieved by means of feeler gauges, are reported in Figure 8. Resolution slots of 0.1 mm cannot be accurately printed along all the recycling steps: this points towards the presence of limitations in terms of SLM technology and the machine parameters. However, after approximately 7x reuses, the 0.2 mm slot became unachievable. This is evidence of small modifications of powder characteristics affecting the overall feedstock lifecycle. When measuring the slots, in cases where a "pass" condition was met, measurements consistently showed negative deviations: this indicates a general under-sizing of each of the measured resolution slots. It is also worth noticing that the smallest thickness deviation of the first few JOBs, characterized by virgin powder or material recycled fewer times, exhibited the largest deviations; however, as the number of reuse cycles increased, error measurements grew in the largest slots as well.

For *resolution holes* (samples ±XH/YH), the inclination evaluations showed positive results in all specimens. No specific trend was identified for a correlation between inclination angle and deviation, as deviations exhibited non-monotonic tendencies across all measurements, varying from one JOB to another.

Concerning *resolution walls* (samples XWR/YWR) both wall planarity and distance between opposite surfaces were evaluated. In **Errore. L'origine riferimento non è stata trovata.**, it can be clearly identified a trend within the results. The distance

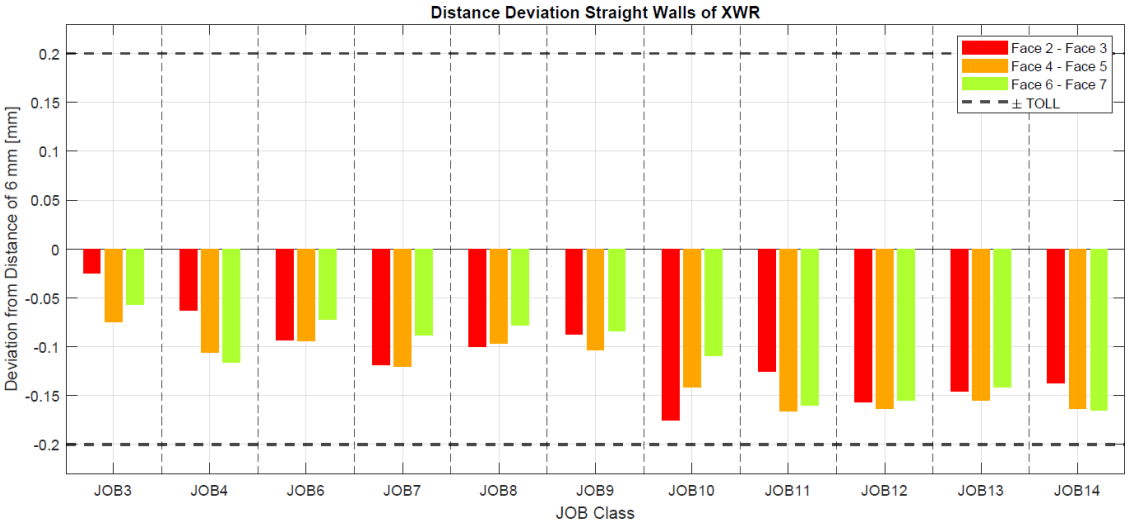

Figure 9: Distance deviations between opposite faces of consecutive walls for XWR.

between the walls is reduced after each recycling cycle, as negative deviations increased; a plateau is therefore reached after JOB10. The cause of this reduction may be attributed to the walls growing thicker than intended. The result can be directly imputed to the phenomenon of recycling of powder which affects the powder properties and therefore the results in terms of final sample dimensions. Nevertheless, despite these deviations, data remained within the tolerance limit of ±0.2 mm across multiple recycling steps. Concerning planarity evaluation on the same feature, no conclusive results were evidenced. This parameter tends to fluctuate across printing cycles, occasionally exceeding the maximum tolerance (even when considering virgin powders), without showing a clear trend.

Considering the *surface texture samples* (XST/YST artefacts), CMM measurements assessed errors in walls inclination, thickness, distance between opposite faces, and distances from the RC to evaluate the machine capability of printing objects in predefined locations.

Inclination results, conducted on the inclined walls relative to the vertical surface of each artefact, revealed errors that varied with both recycling cycles and orientation. Instability of the first two inclined walls, which were the thinnest among the printed ones (0.2mm and 0.4mm respectively), was registered in the results independently from the printing cycle. On these samples, errors exceeding the tolerances of ±0.5° were registered, mainly due to the limitation of the AM machine to print overhanging surfaces with thickness values lower than 0.4 mm. The same instability was noted in the thickness measurements, as these thin walls often surpassed the maximum allowable error. Consequently, the distance between opposite faces on these walls, intended to be 6.0 mm, turned out to be out of tolerance (usually undersized). Nonetheless, no clear trend was registered on the remaining inclined walls, which could be directly imputed to the powder recycling methodology and corresponding recycling steps.

5.4 Surface Roughness Results

Surface roughness measurements were recovered from all test cube artefacts at varying degrees of powder recycling. First, surface roughness was determined on the straight back walls of X/YST thanks to their suitability in collecting data for areal Ra measurements following the parameters outlined by the guidelines. The trend in Figure 10 reveals a progressive, yet non-monotonic, increase as the powder is reused, rising from an average of 6.887 µm in JOB3 (virgin) to an average of 13.313 µm in JOB15 (11x recycled).

Variability in Ra evolution was also observed in the other test cube artefacts: sometimes, samples produced with IN718 recycled a specific number of times exhibited lower roughness values compared to to those from earlier printing cycles.

Figure 11 illustrates the results when considering the combined influence of factors such as material reuse, thickness, and inclination. For the same inclination, roughness tends to decrease as thickness increases, while the opposite trend was observed when thickness remained constant. However, each JOB exhibited a distinct roughness profile, with the highest values generally found for increased recycling steps, though not consistently.

A theoretical model, proposed by Reeves and Cobb [20] and valid for inclined surfaces was used to predict surface roughness. The model is expressed through the equation (3) where δ denotes the layer thickness and θ the inclination angle:

$$Ra = \frac{\delta}{4}\cos\theta \tag{3}$$

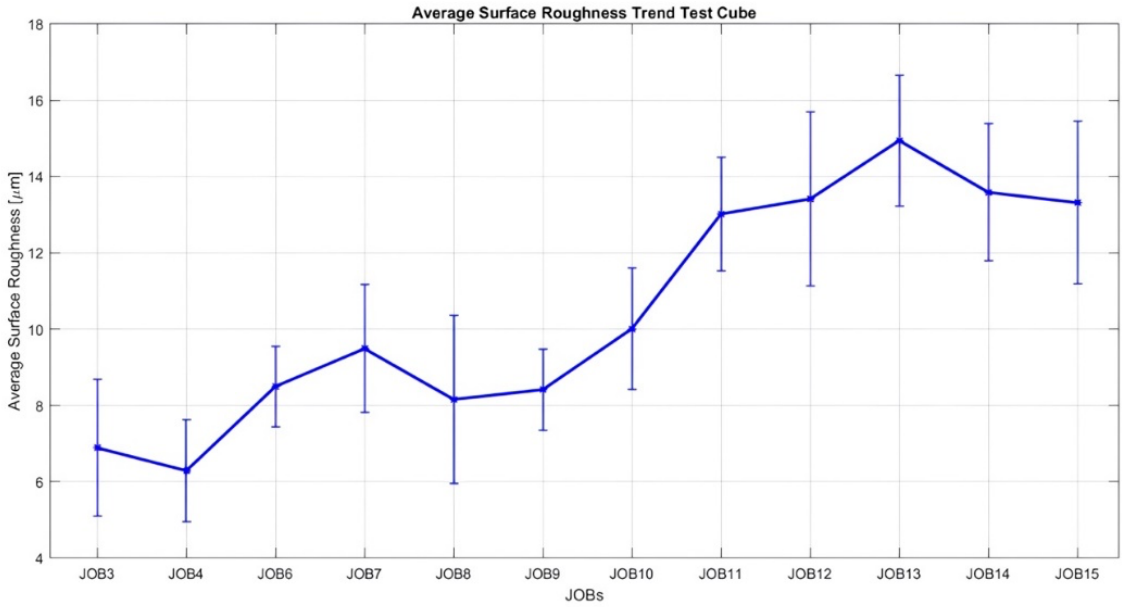

Figure 10: Average surface roughness trend with powder recycling.

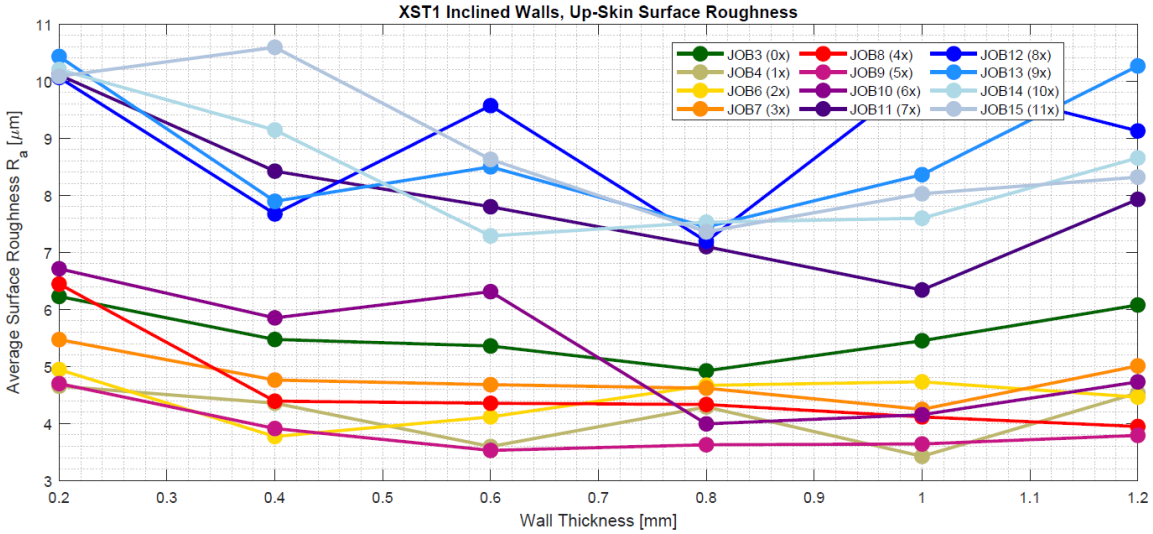

Figure 11: Average surface roughness versus wall thickness for XST1 artefact, upskin results.

As it is reported in Figure 12, the expected results seem not to match the actual measurements. The discrepancy is even more pronounced when dealing with downskin surfaces. The presence of this gap can be attributed to the oversimplified nature of the model, which does not account for factors such as the difference between upskin and downskin surfaces, the staircase effect, production imperfections, or the impact of recycled powder.

One of the most challenging factors which affect the surface roughness result in these samples can be imputed to the staircase effect.

This phenomenon can be clearly recognized in downward-facing surfaces results: due to the layer deposition mechanism, small steps are formed along the process, exposing more surface area to the surrounding particles; then, when the laser generates a melt pool, the thermal energy distributes within the powder bed and is transferred to the adjacent particles and the material which has already being solidified in a different way, leading to a further accentuating effect on the downskin with respect to upskin [21].

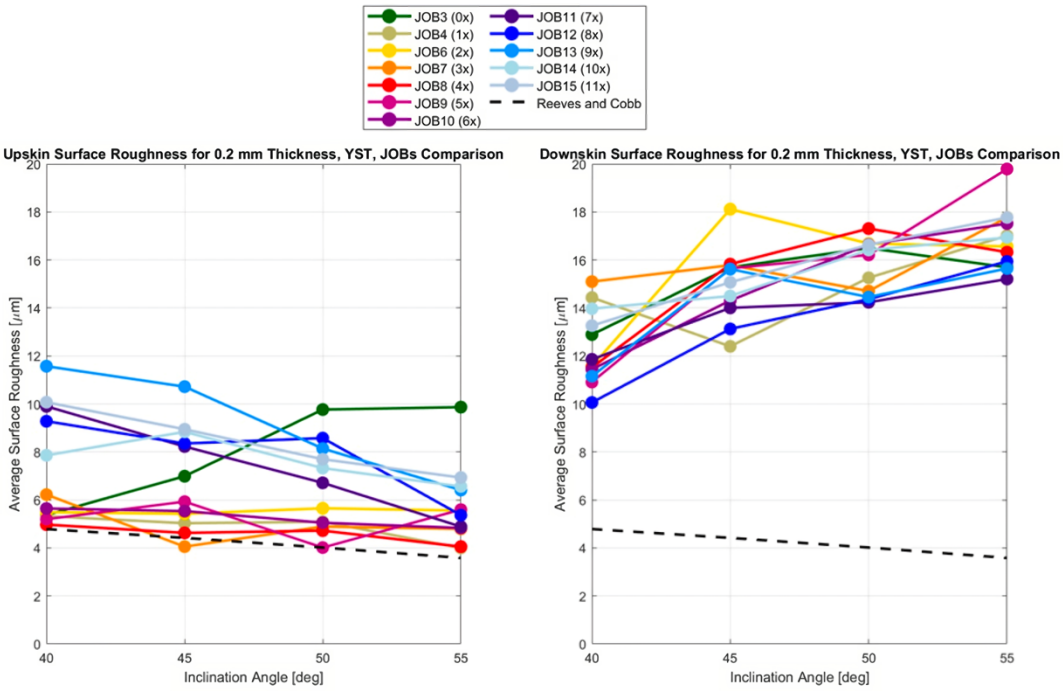

Figure 12: Average surface roughness vs inclination for 1.0 mm wall thickness, YST.

This effect is clear when comparing upskin and downskin surface roughness results for the same object (see Figure 13 and Figure 14 respectively).

The impact of recycling steps on surface roughness due to the wall inclination is clearly affected by the thermal dissipation along the material and the staircase effect. This is confirmed by the analysis of the surface roughness on inclined walls of XRS/YRS samples, which only include upskin surfaces and very small inclinations (between 0° and 30° from the printing plane). Figure 15 reports the results of these data, where no clear impact of recycling phenomena on surface roughness is evidenced. The average values at different inclinations are confirming the results from the upskin area measurements taken from the inclined wall samples.

In order to evaluate the dependence of the surface roughness variation with recycling steps and the wall thickness on avoiding the presence of the staircase effects of the overhanging angle surfaces, measurements on the straight walls of X/YRW artefacts were performed. Furthermore, the impacts on Ra between opposite faces of the same wall due to thermal dissipation were considered. Figure 16 and Figure 17 illustrate additional roughness trends with multiple recycling cycles. Larger thicknesses were always associated with the highest measured values of surface roughness, though the increase was rarely monotonic. Typically, the maximum roughness was achieved by the middle walls, particularly 0.4 mm, probably due to particles compaction between walls whose distance – as depicted by the dimensional errors analysis – was slightly undersized.

6 Conclusions and Future Developments

Within this work, an analysis of AM SLM samples printed with IN718 material across multiple recycling steps was performed. A unique layout was selected for the printing job and multiple samples followed a specific AM procedure and a dedicated tailored AM plan, as retrieved from standards. The analysis covered a series of samples for tensile and metallographic tests as well as dedicated secondary artefact retrieved from the "test cube" printing artefact for dimensional and surface roughness measurements across printing jobs.

The results of the analyses revealed specific trends, reflecting the behaviours associated with altered powder particles material properties. No significant detrimental impacts on mechanical properties were registered when considering tensile samples and metallographic specimens for densification analysis. Furthermore, coherence was observed relative to geometrical and dimensional values. Large secondary artefact retrieved from the test cube, such as thick walls and large cylinders, exhibited lower errors and greater stability, independently on the recycling cycle. Surface roughness variations in function of the geometry were considered, and microstructural changes occurred progressively with powder reuse. In particular, significant impact of the staircase effect on overhanging surfaces and its contribution towards surface roughness degradation across recycling steps was registered, in particular on downskin areas.

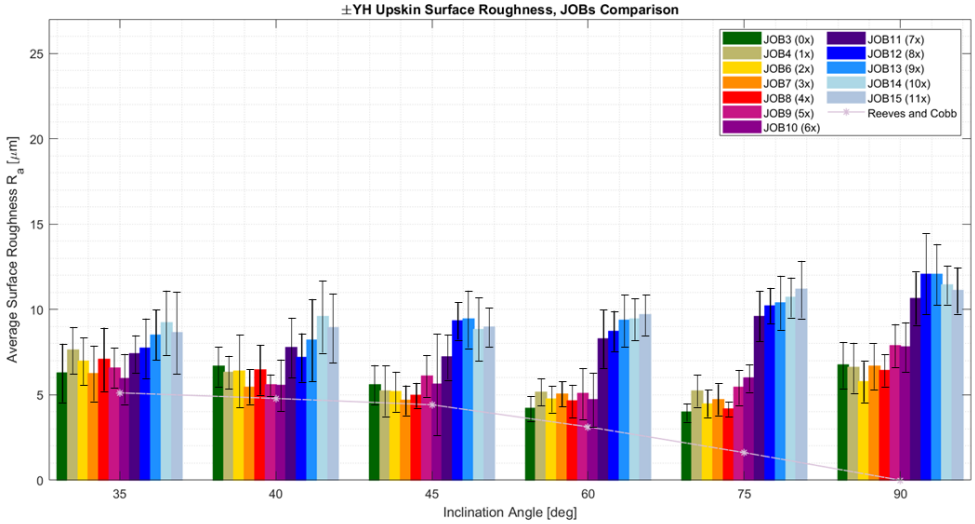

Figure 13: YH upskin average surface roughness.

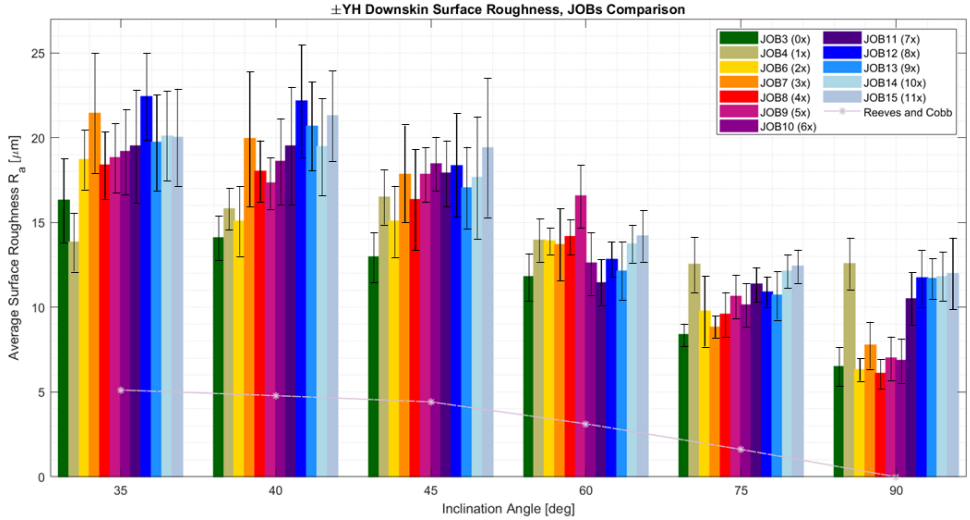

Figure 14: YH downskin average surface roughness.

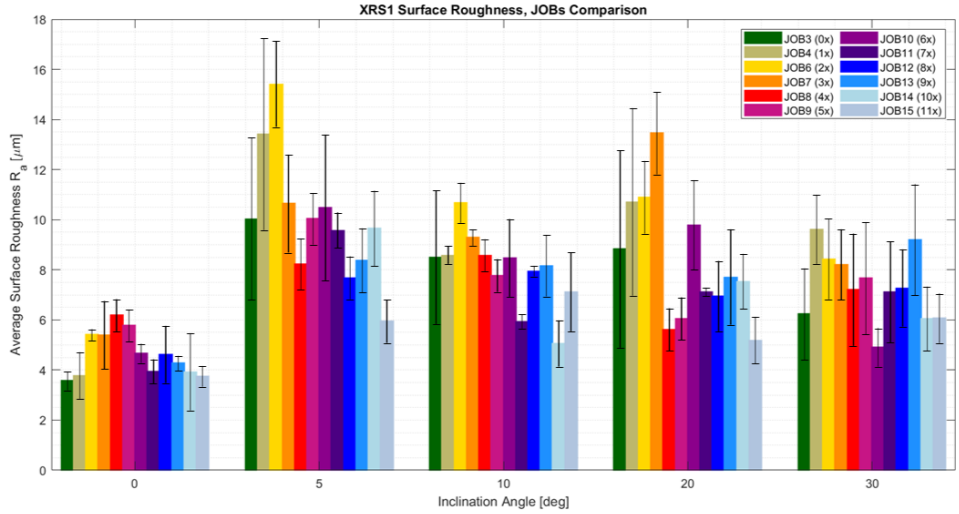

Figure 15: XRS1, Ra at different inclinations.

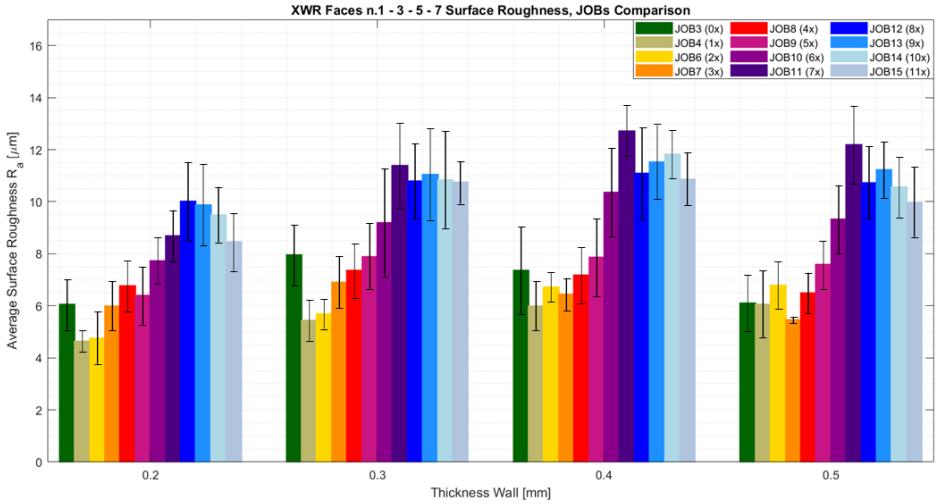

Figure 16: XWR, Ra on different faces (1-3-5-7).

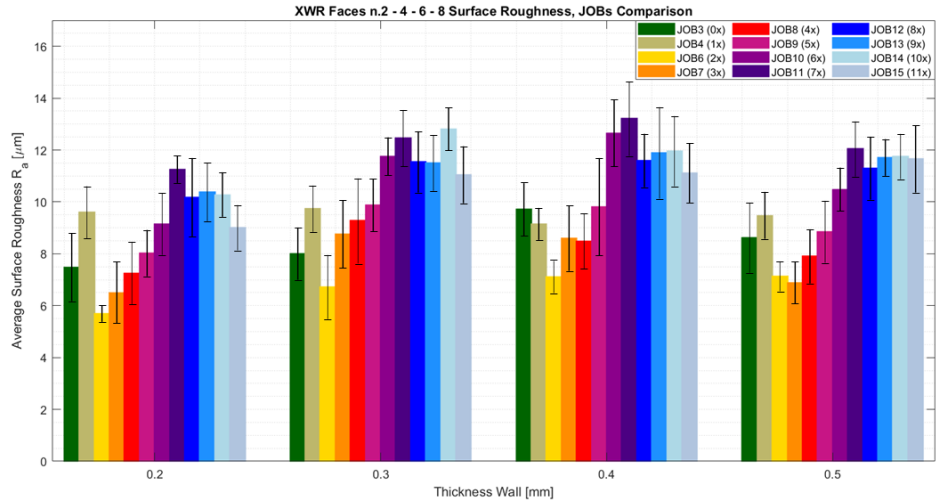

Figure 17: XWR, Ra on different faces (2-4-6-8).

Despite the unpredictability, most probably due to particles movement during distribution on the building plate and modification at rheological properties level across recycling, the results remained quite consistent, with no drastic deviations between samples. This suggests that recycling did not remarkably compromise the accuracy, the surface texture, the microstructural aspects or the mechanical properties of an object, when comparing its counterpart produced through virgin powder.

As future developments, limitations in terms of maximum recycling step allowed as well as feasible geometries and adjustments to the process parameters will be integrated in the design as limitations retrieved from the SLM process and the recycling steps applied.

Further analyses including the postprocessing of internal channels printed in the test cube across recycled powders shall be considered and integrated in the analyses. This would allow to optimize the SLM machine and the production of samples for altered feedstock, ensuring repeatability of results and operational efficiency of machines across multiple printing steps.

Acknowledgements

The author acknowledges D-Orbit SpA company for the support in providing the samples needed to perform the proposed research work.

Appendix A

Table 5: JOBs organization and characteristics.

Phase	JOB	Powder	Sample
Pre Verification	JOB0	Virgin	- 60 cubic samples
	JOB0.1		- 36 inclined walls samples
	JOB0.2		
	JOB1		- 27 cylindrical samples - 9 cubic specimens - 9 rectangular samples - 1 powder sample cone
	JOB1.1		- 24 rectangular samples
AM Verification	JOB2		- 46 cylindrical samples - 2 rectangular specimens - 1 powder sample cone
	JOB3		- 35 cylindrical samples - 2 rectangular samples - 1 Test cube
Proto Verification	JOB4	1x Recycl	- 15 cylindrical samples - 2 rectangular samples - 1 powder sample cone - 1 Test cube
	JOB5		
	JOB6	2x Recycl	
	JOB7	3x Recycl	
	JOB8	4x Recycl	
	JOB9	5x Recycl	
	JOB10	6x Recycl	
	JOB11	7x Recycl	
	JOB12	8x Recycl	
	JOB13	9x Recycl	
	JOB14	10x Recyc	
	JOB15	11x Recyc	

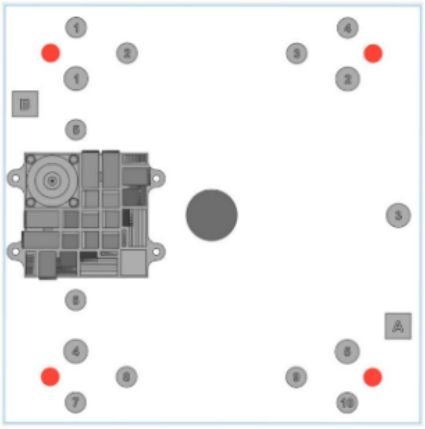

Figure 18: Example of JOB6 to JOB14 machine layout. Cylindrical samples are distributed on the plate together with rectangular samples (top left and bottom right), test cube (center left) and powder collection cone (center).

References

[1] Herzog, D., Seyda, V., Wycisk, E., & Emmelmann, C. (2016). Additive manufacturing of metals. *Acta Materialia*, *117*, 371-392.

[2] Gibbons, D. W., Govender, P., & van der Merwe, A. F. (2024). Metal powder feedstock evaluation and management for powder bed fusion: a review of literature, standards, and practical guidelines. *Progress in additive manufacturing*, *9*(4), 805-833.

[3] Moghimian, P., Poirié, T., Habibnejad-Korayem, M., Zavala, J. A., Kroeger, J., Marion, F., & Larouche, F. (2021). Metal powders in additive manufacturing: A review on reusability and recyclability of common titanium, nickel and aluminum alloys. *Additive Manufacturing*, *43*, 102017.

[4] Dr. Proof, H., Challenges of Additive Manufacturing: Why companies don't use Additive Manufacturing in serial production, 28 July 2019, Challenges of Additive Manufacturing | Deloitte Deutschland (accessed 20.09.24).

[5] Kumar, M. B., & Sathiya, P. (2021). Methods and materials for additive manufacturing: A critical review on advancements and challenges. *Thin-Walled Structures*, *159*, 107228.

[6] Ghidini, T., Grasso, M., Gumpinger, J., Makaya, A., & Colosimo, B. M. (2023). Additive manufacturing in the new space economy: Current achievements and future perspectives. *Progress in Aerospace Sciences*, 100959.

[7] Gradl, P., Tinker, D. C., Park, A., Mireles, O. R., Garcia, M., Wilkerson, R., & Mckinney, C. (2022). Robust metal additive manufacturing process selection and development for aerospace components. *Journal of Materials Engineering and Performance*, *31*(8), 6013-6044.

[8] Ghidini, T., Additive Manufacturing for Space and Aerospace Applications, Lecture Notes, Politecnico di Milano, 2023.

[9] ECSS-Q-ST-70-80C – Processing and quality assurance requirements for metallic powder bed fusion technologies for space applications, 11 August 2021, ECSS-Q-ST-70-80C – Processing and quality assurance requirements for metallic powder bed fusion technologies for space applications (30 July 2021) | European Cooperation for Space Standardization (accessed 20.09.24).

[10] ISO/ASTM 52902:2019(E), Additive manufacturing – Test artefacts – Geometric capability assessment of additive manufacturing systems, Edition 2, 2023.

[11] ASTM E8/E8M-22, Standard Test Method for Tensile Testing of Metallic Materials, 5 March 2024 E8/E8M Standard Test Methods for Tension Testing of Metallic Materials (astm.org) (accessed 20.09.24).

[12] ISO 6892-1:2019 Metallic materials — Tensile testing, Part 1: Method of test at room temperature, Edition 3, 2019.

[13] ASTM B311-17, Standard Test Method for Density of Powder Metallurgy (PM) Materials Containing Less Than Two Percent Porosity, ASTM B311-17 - Standard Test Method for Density of Powder Metallurgy (PM) Materials Containing Less Than Two Percent Porosity (ansi.org), 13 September 2022 (accessed 20.09.24).

[14] ASTM E3-11. (2017), Standard guide for preparation of metallographic specimens. *ASTM International: West Conshohocken, PA, USA*.

[15] American Society for Testing and Materials. (2023). *ASTM E 407-23: Standard Practice for Microetching Metals and Alloys*, 21 November 2023, E407 Standard Practice for Microetching Metals and Alloys (astm.org) (accessed 20.09.24).

[16] BS EN ISO 3274:1998, Edition 2, 1998.

[17] Gibson, I., Rosen, D. W., Stucker, B., Khorasani, M., Rosen, D., Stucker, B., & Khorasani, M. (2021). *Additive manufacturing technologies* (Vol. 17, pp. 160-186). Cham, Switzerland: Springer.

[18] Kalami, H., & Urbanic, J. (2021). Exploration of surface roughness measurement solutions for additive manufactured components built by multi-axis tool paths. *Additive Manufacturing*, *38*, 101822.

[19] Yi, F., Zhou, Q., Wang, C., Yan, Z., & Liu, B. (2021). Effect of powder reuse on powder characteristics and properties of Inconel 718 parts produced by selective laser melting. Journal of Materials Research and Technology, 13, 524-533.

[20] Strano, G., Hao, L., Everson, R. M., & Evans, K. E. (2013). Surface roughness analysis, modelling and prediction in selective laser melting. *Journal of Materials Processing Technology*, *213*(4), 589-597.

[21] Sanaei, N., & Fatemi, A. (2021). Defects in additive manufactured metals and their effect on fatigue performance: A state-of-the-art review. *Progress in Materials Science*, *117*, 100724.